OPTOSKY
Spectroscopy Solutions

Datasheet

MIR Hyperspectral Imager ATH1080

Features

- Wavelength Range: 2.5~5.0 μm, 7.8~12.3 μm
- Spectral Path: Holographic Transmission Grating
- Ultra-Low-Temperature Stirling-Cooled CCD
- Detector Resolution: 640x512 or 320x256
- Advanced Image Compression Algorithm
- Compact Size: 279 mm × 135 mm × 145 mm
- Lightweight: <4500 g
- No Mechanical Scanning, High Reliability

Application

- Geological and Mineral Resource Exploration
- Precision Agriculture, Crop Growth and Yield Assessment
- Forest Pest and Disease Monitoring, Fire Prevention Monitoring
- Coastline and Marine Environment Monitoring
- Grassland Productivity and Monitoring
- Lake and Watershed Environment Monitoring
- Remote Sensing Education and Research
- Meteorological Research
- Ecological Environmental Protection and Mining Environment Monitoring
- Water Quality Testing, Soil Monitoring
- Agricultural and Livestock Product Quality Testing
- Military, Defense, and National Security
- Disaster Prevention and Control

Description

The ATH1080 is a hyperspectral imager specifically designed by Optosky for the mid- to far-infrared spectral bands. In addition to being compact and lightweight, the ATH1080 uses a Stirling-cooled CCD with deep cooling, featuring low dark current, low noise, high spatial resolution, high spectral resolution, and a wide imaging range. The ATH1080 consists of two main components: an imaging lens and a hyperspectral spectrometer. The hyperspectral spectrometer is based on transmission grating technology, which provides excellent aberration characteristics.

The ATH1080 utilizes a Stirling deep-cooled high-performance infrared CCD imaging device, offering clear images with minimal noise. The ATH1080 is a conventional straight-tube hyperspectral camera, suitable for multi-rotor camera drones and agriculture drones. For fixed-wing camera drones and other drones with short landing gear, Optosky has developed the specialized ATH1080L model with a bent optical path, reducing the height requirements for landing gear.

The ATH1080 can be used for real-time measurement of spectral information from various ground features such as plants, water bodies, and soil, obtaining spectral images. By analyzing these spectral images, relationships can be established with the physical and chemical properties of plants and other features, useful for plant classification, monitoring plant growth conditions, and other research. The entire system is compactly designed, with the main spectrometer unit offering high spectral resolution. It employs an external push-broom imaging method, which can be integrated with field rotary platforms and indoor linear scanning platforms to form independent measurement systems. Additionally, it can be mounted on drones for aerial remote sensing operations, contributing to agricultural production and environmental monitoring.

Model	Features
ATH1080-MW	2.5~5.0 μm, Stirling Cooled
ATH1080-LW	7.8~12.3 μm, Stirling Cooled

Figure 1 ATH1080-K Hyperspectral Imager (Core: ATH1080)

1503 Bld. A04, 3rd Software Park, Jimei, Xiamen, 361005, China
Tel: +86-592-6102588

1. Selection Guide

Model	Features
ATH1080-MW-MCT3	2.5~5.0 μm, 320x256, Stirling Cooled MCT Detector
ATH1080-MW-MCT6	2.5~5.0 μm, 640x512, Stirling Cooled MCT Detector
ATH1080-LW-MCT3	7.8~12.3 μm, 320x256, Stirling Cooled MCT Detector
ATH1080-LW-MCT6	7.8~12.3 μm, 640x512, Stirling Cooled MCT Detector

2. Parameter

No.	Specification	**ATH1080-MW**	**ATH1080-LW**
1	Spectral Range	2.5~5.0μm	7.8~12.3μm
2	Spectral Resolution (FWHM)	No Binning：<30nm 4X4binning：50nm	No Binning：<50nm 4X4binning：100nm
3	Sampling Interval	8.0 nm	15.0 nm
4	F/#	F/2.6	F/2.6
5	Sensor	Stirling Cooled MCT CCD	Stirling Cooled MCT CCD
6	Data interface	USB3.0	USB3.0
7	Power Consumption	DC12V，<15 W	DC12V，<15W
8	Sensor Size	9.6 mm × 7.68 mm	9.6 mm × 7.68 mm
9	Sensor Resolution	ATH1080-MW-MCT3：320×256 ATH1080-MW-MCT6：640×512	ATH1080-LW-MCT3：320×256 ATH1080-LW-MCT6：640×512
10	Pixel Size	ATH1080-MW-MCT3：30μm ATH1080-MW-MCT6：15μm	ATH1080-LW-MCT3：30μm ATH1080-LW-MCT6：15μm
11	Bit Depth	16 bits	16 bits
12	NETD	<20mK	<1K
13	Dynamic range	73 dB	60 dB
14	Slit Width	30μm、15μm	30μm、15μm
15	Binning Mode	4×4 / 2×4	4×4 / 2×4
16	Max spatial Bands	256、512	256、512
17	Max Spectral Bands	320、640	320、640
18	(FOV)	12.5°@f=35 mm 17.5°@f=25 mm	12.5°@f=35 mm 17.5°@f=25 mm
19	(IFOV)	0.017mrad @ f=35 mm 0.0234mrad @f=25 mm	0.00977mrad@f=35 mm 0.0137mrad@f=25mm
20	Max Frame Rate	150 fps	120 fps
21	Dimensions	279 mm × 135 mm × 145 mm	279 mm × 135 mm × 145 mm

1503 Bld. A04, 3rd Software Park, Jimei, Xiamen, 361005, China
Tel: +86-592-6102588

22	Weight	<3545 g	<3580 g
23	Operating Temperature	-20 ~ 50°C	
24	Storage Temperature	-30 ~ 70°C	
Note: The parameters in the table are for reference only; other performance parameters of the instruments can be customized.			

Note:
1: This value is measured under 4x4 binning conditions. The binning operation can improve the signal-to-noise ratio.
2: The field of view (FOV) and instantaneous field of view (IFOV) are determined by the imaging lens. The values in the table are measured with a 25 mm focal length lens. Imaging lenses with different focal lengths, such as 15 mm, 18 mm, and 35 mm, can be used to obtain different FOV and IFOV.

3. Imaging Test of ATH1080

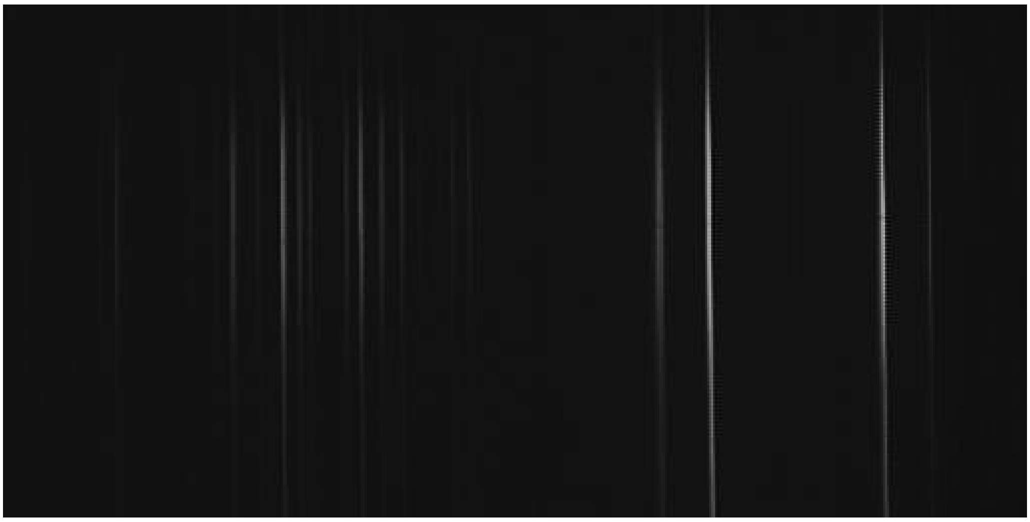

Figure 2 Spectral Image Captured by ATH1080

4. ATH1080 Physical and Dimensional Diagram

1503 Bld. A04, 3rd Software Park, Jimei, Xiamen, 361005, China
Tel: +86-592-6102588

Figure 3 ATH1080K/ATH1080KW Hyperspectral Imagers (Core: ATH1080 and ATH1080W, respectively)

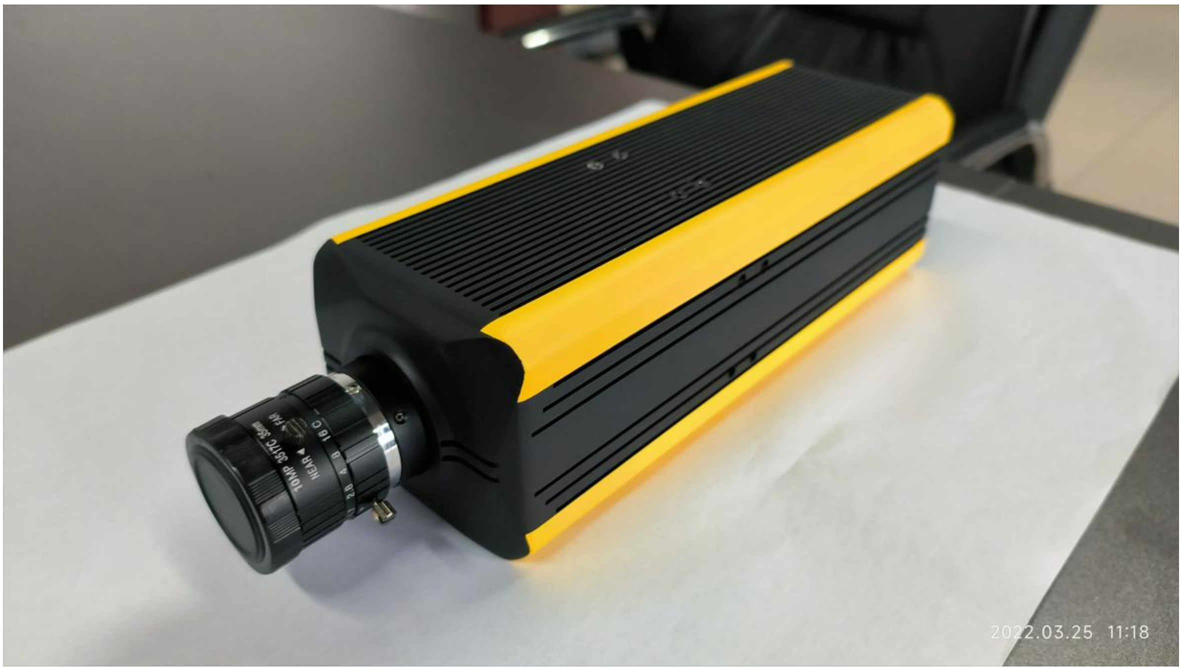

1503 Bld. A04, 3rd Software Park, Jimei, Xiamen, 361005, China
Tel: +86-592-6102588

Figure 4 ATH1080K/ATH1080KW Hyperspectral Imager

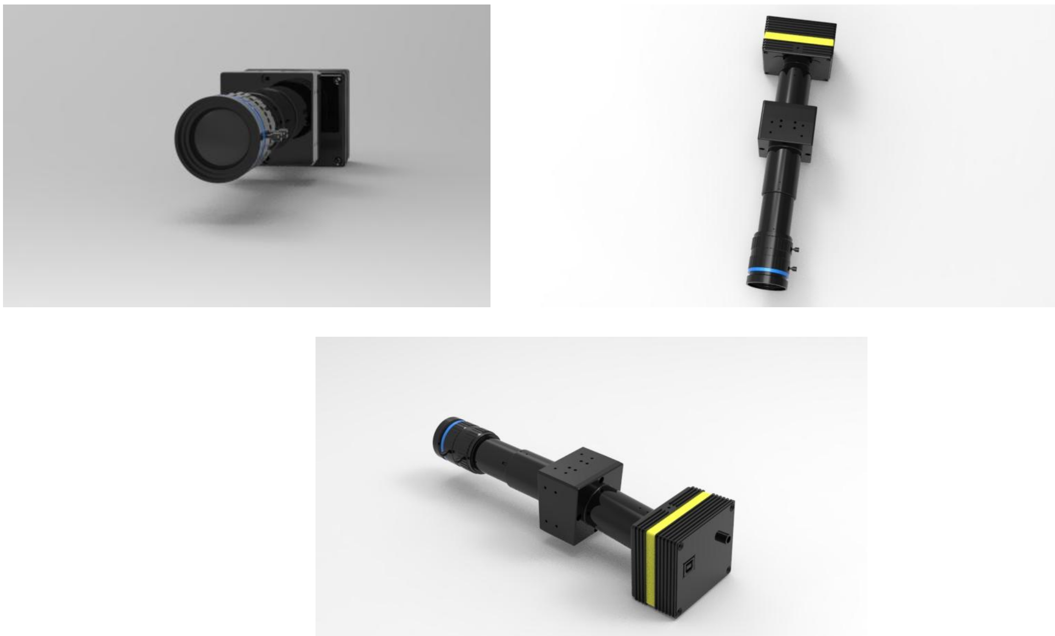

Figure 5 ATH1080 Appearance Design Diagram

1503 Bld. A04, 3rd Software Park, Jimei, Xiamen, 361005, China
Tel: +86-592-6102588

5. Application Examples

Figure 14 UAV Mounting Experiment

1503 Bld. A04, 3rd Software Park, Jimei, Xiamen, 361005, China
Tel: +86-592-6102588

Figure 15 Field Experiment Scene 1

Figure 16 Field Experiment Scene 2

1503 Bld. A04, 3rd Software Park, Jimei, Xiamen, 361005, China
Tel: +86-592-6102588

Figure 17 Field Experiment Scene 3

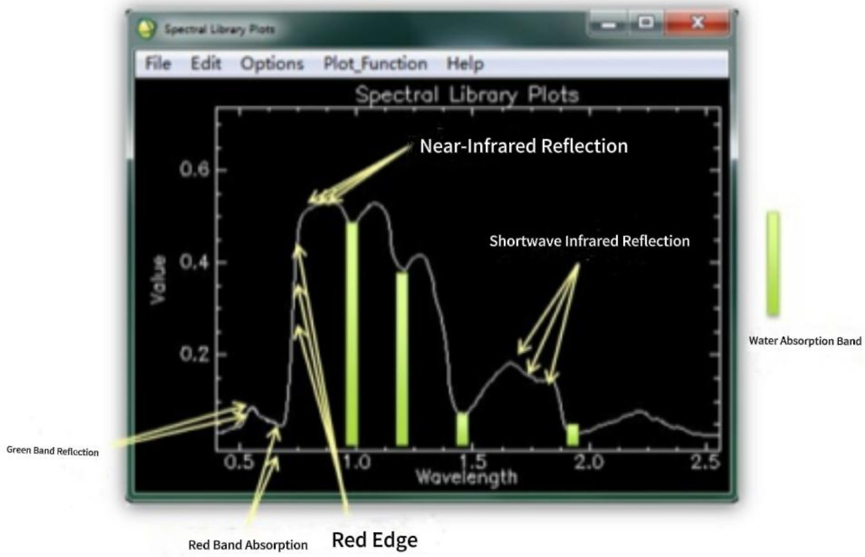

Figure 18 Hyperspectral Imager Spectral Image of Green Plants

5.1. Application in Mineral Exploration

Spectral remote sensing technology evolved from multispectral remote sensing technology represented by Landsat, initially taking shape in the mid-1980s (Goets et al., 1985; Tong Qingxi et al., 2006). Due to its high spectral resolution and integrated imaging capabilities, hyperspectral remote sensing technology offers the ability to detect and analyze surface rock and mineral compositions at large spatial scales. It can provide not only macroscopic ground images but also determine the types and abundances of minerals within geological bodies at the pixel level, and even some chemical compositions of certain minerals (Wang Runsheng et al., 2010). In recent years, with the continuous development of hardware, data processing methods, and software related to imaging spectrometers, the application of hyperspectral remote sensing technology in geological surveys has accelerated. From large mineralization belts to medium-sized mineral fields, hyperspectral remote sensing technology has played a significant role in geological mapping, defining and delineating hydrothermal alteration zones, and identifying and characterizing mineralization anomalies (e.g., Bierwirth et al., 2002; Lian Changyun et al., 2005; Kruse et al., 2006; Cudahy et al., 2007; Wang Runsheng et al., 2010; Liu Dechang et al., 2011; Yan Baikun et al., 2014; Yang Zi'an et al., 2015; Graham et al., 2017). As the theory of mineralization systems (Wyborn et al., 1994) becomes more deeply integrated into exploration practice, specialized mineral mapping at the scale of large mineral clusters and mineralization belts will provide key regional material composition information for predictive exploration.

The spectral wavelength ranges used for mineral mapping include visible light (400~700 nm), near-infrared (700~1000 nm), shortwave infrared (1000~2500 nm), and thermal infrared (7000~15000 nm). Currently, the most widely used range in mining applications is the shortwave infrared region (1000~2500 nm). Due to its proximity to the frequencies of vibrational and combination bands of chemical bonds in mineral lattices, the shortwave infrared wavelength range can observe minerals containing water or OH- (mainly layered silicates and clays) as well as certain sulfates and carbonates.

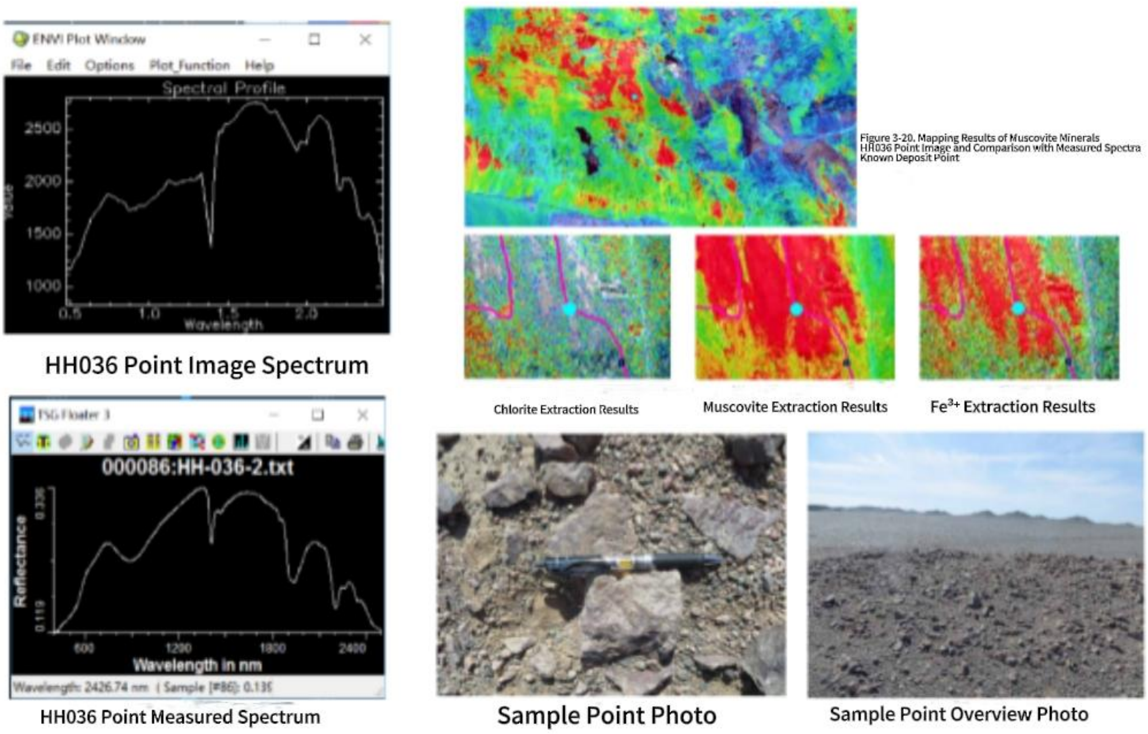

1503 Bld. A04, 3rd Software Park, Jimei, Xiamen, 361005, China
Tel: +86-592-6102588

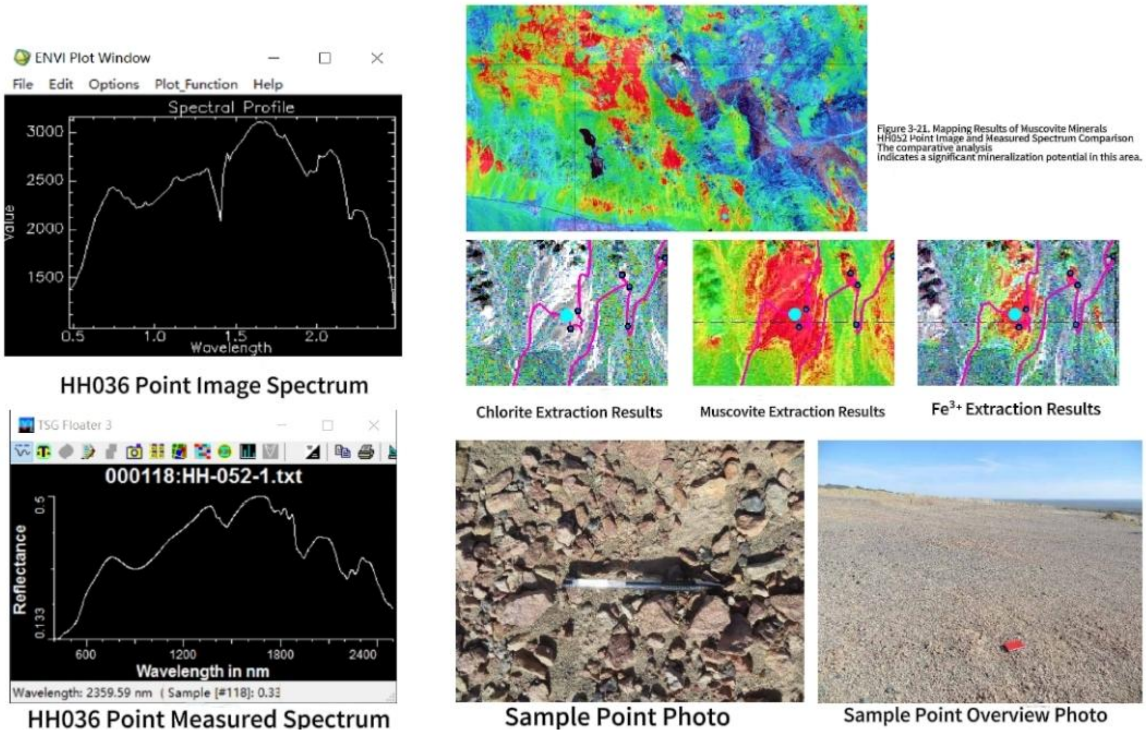

Figure 19 Application of Hyperspectral Imager in Mineral Exploration

Soil salinization is one of the major ecological and environmental issues faced by arid and semi -arid regions. The consequences of soil salinization, such as soil hardening, decreased fertility, p H imbalances, and land degradation, severely restrict agricultural development in China and imp act the overall strategy for sustainable development. Remote sensing technology, with its large s cale, broad range, timeliness, and cost-effectiveness, addresses the shortcomings of traditional mo nitoring methods for salinization and provides a novel approach for the quantitative monitoring of soil salinization.

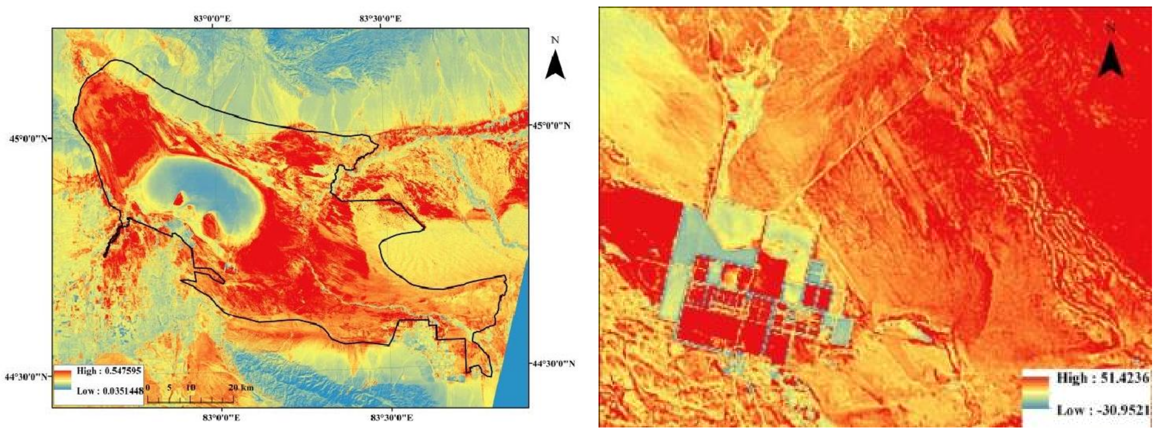

Figure 20 Surrounding Area of a Salt Field

1503 Bld. A04, 3rd Software Park, Jimei, Xiamen, 361005, China
Tel: +86-592-6102588

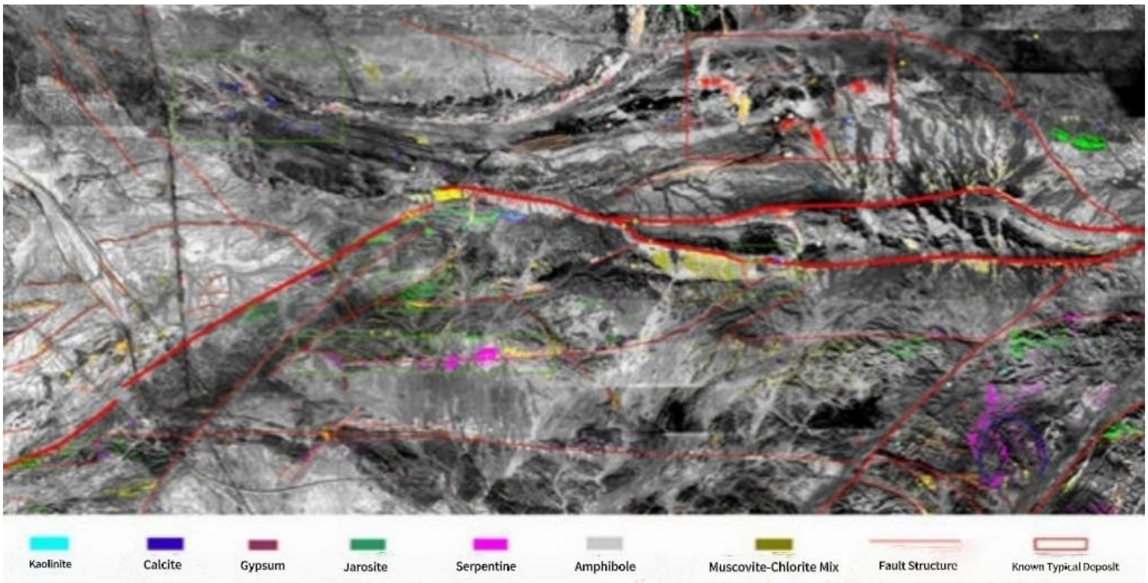

Figure 21 Measurement Diagram of a Mine Site

5.2. Application in Vegetation Growth Monitoring

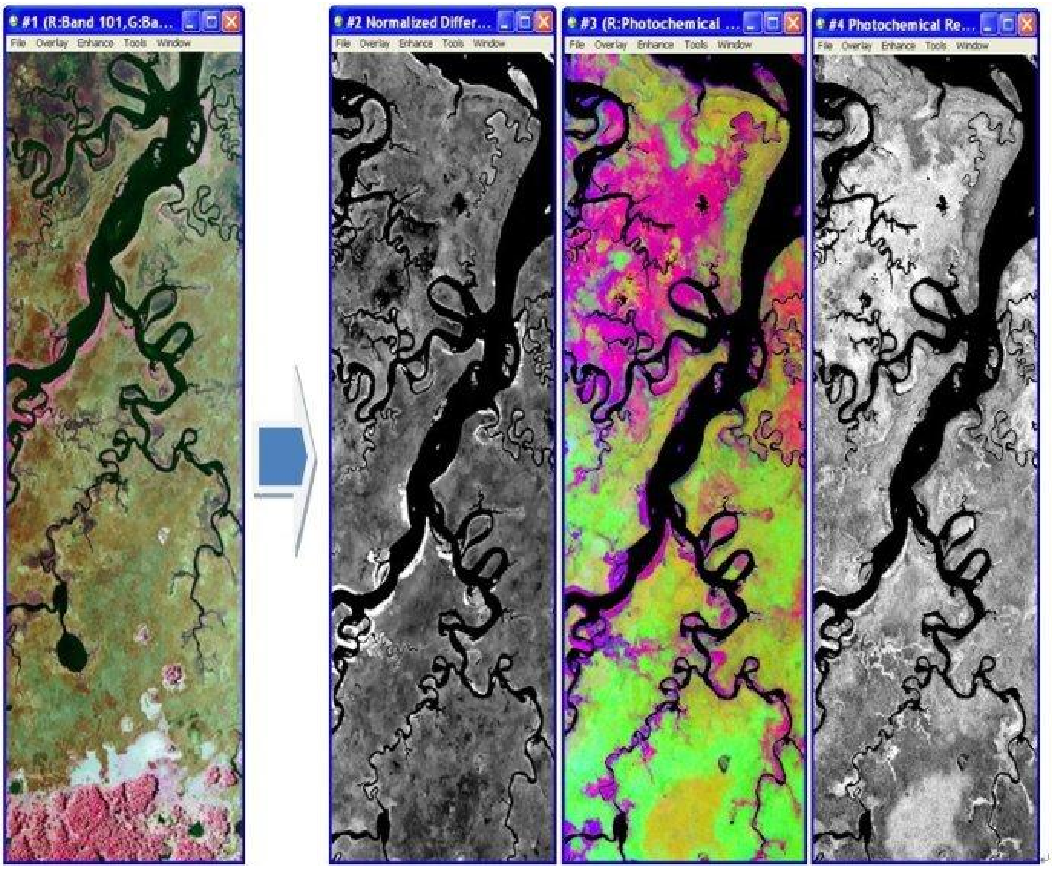

Figure 22 Hyperspectral Image of Vegetation Growth

1503 Bld. A04, 3rd Software Park, Jimei, Xiamen, 361005, China
Tel: +86-592-6102588

5.3. Application in Forest Health Monitoring

Used for pest and disease monitoring, forest resource assessment

Principle: The health of vegetation is related to the greenness index, leaf area index, leaf moisture content, and light use efficiency.

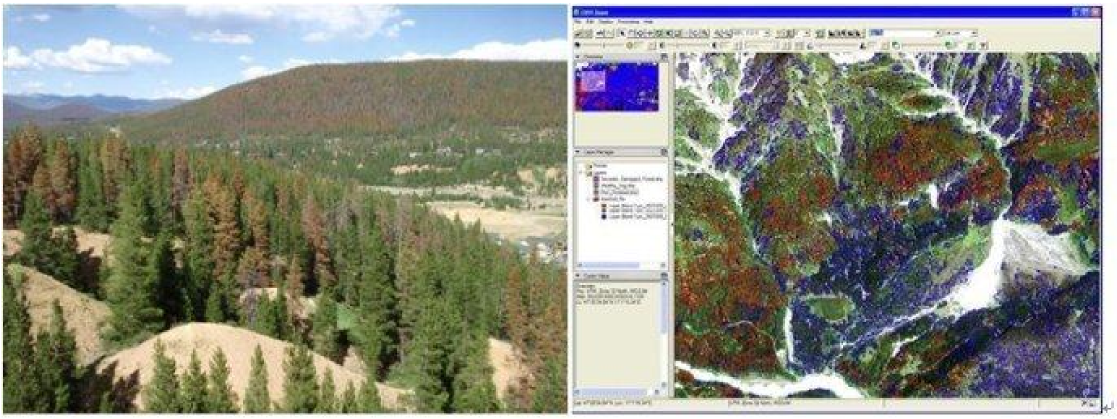

Figure 23 Hyperspectral Imager Researching the Health of Pinus Massoniana

5.4. Application in Forest Fire Prevention

Fire Risk Analysis Identifying potential fire zones and ignition points

Principle :The likelihood of vegetation fire is related to the greenness index, canopy moisture content, drought c onditions, and carbon loss caused by non-photosynthetic plants.

1503 Bld. A04, 3rd Software Park, Jimei, Xiamen, 361005, China
Tel: +86-592-6102588

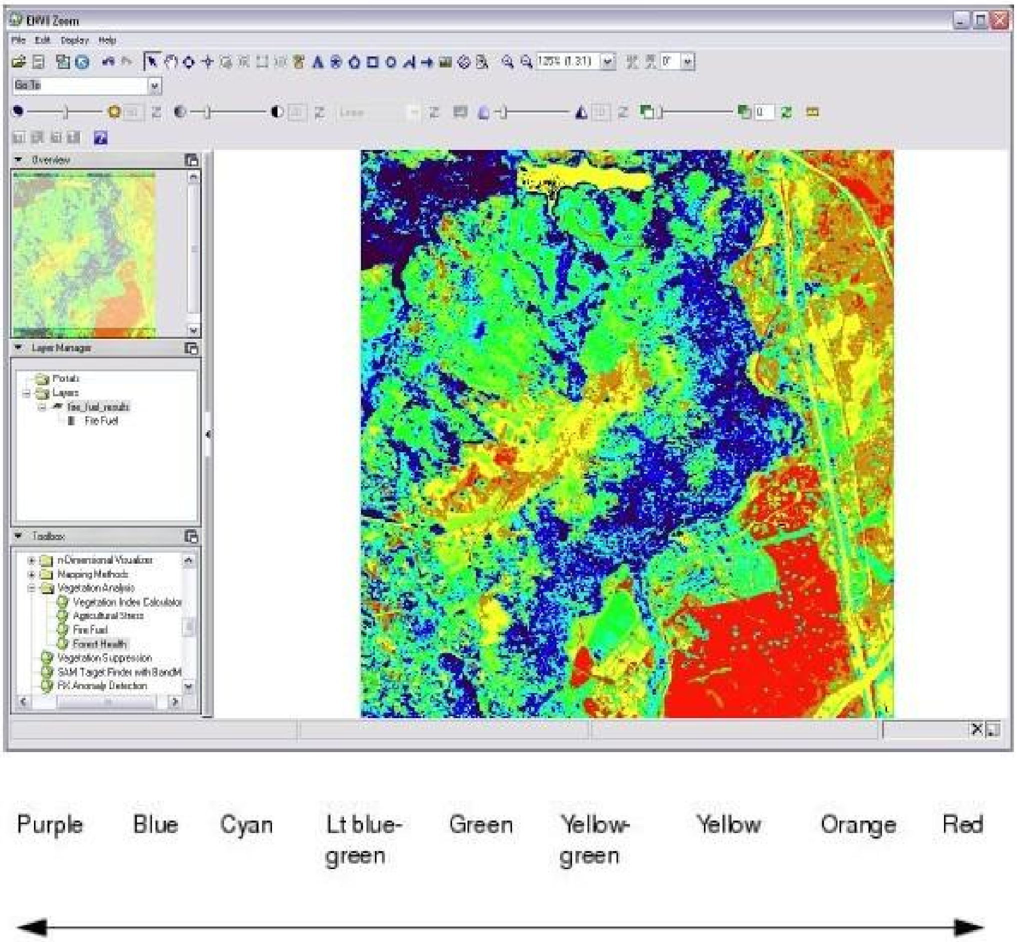

Figure 24 Application of Hyperspectral Imaging in Forest Fire Prevention

5.5. Application in Medical Microscopic Spectral Imaging

Application Goal: Intraoperative online detection and navigation for tumor surgery

1503 Bld. A04, 3rd Software Park, Jimei, Xiamen, 361005, China
Tel: +86-592-6102588

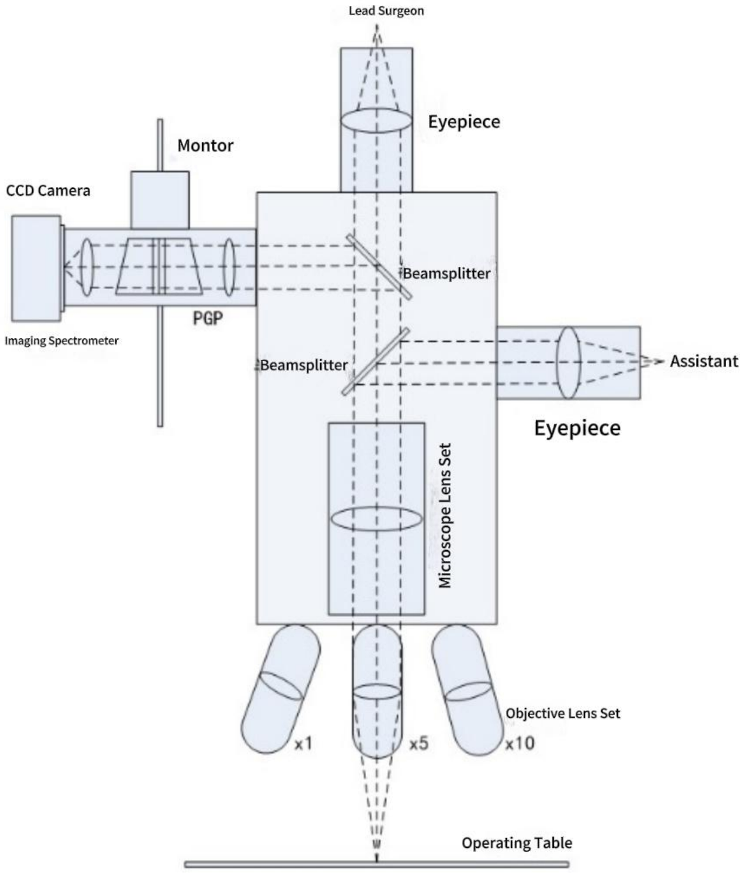

Figure 25 Schematic Diagram of Optical Path for Medical Microscopic Spectral Imager

The figure shows the principle schematic of a medical microscopic spectral imager. The target to be examined o n the operating table is divided into three paths after passing through the objective lens and microscope lens gr oup: one path is for the primary surgeon's visual observation, another path is for the assistant's visual observatio n, and the third path is detected and received by the imaging spectrometer. The imaging spectrometer, driven by a motor, performs spatial scanning of the target to obtain imaging spectral information. After data analysis and image processing, the results are displayed to the doctor via a monitor.

1503 Bld. A04, 3rd Software Park, Jimei, Xiamen, 361005, China
Tel: +86-592-6102588

Figure 26 Physical Image of Medical Microscopic Spectral Imager

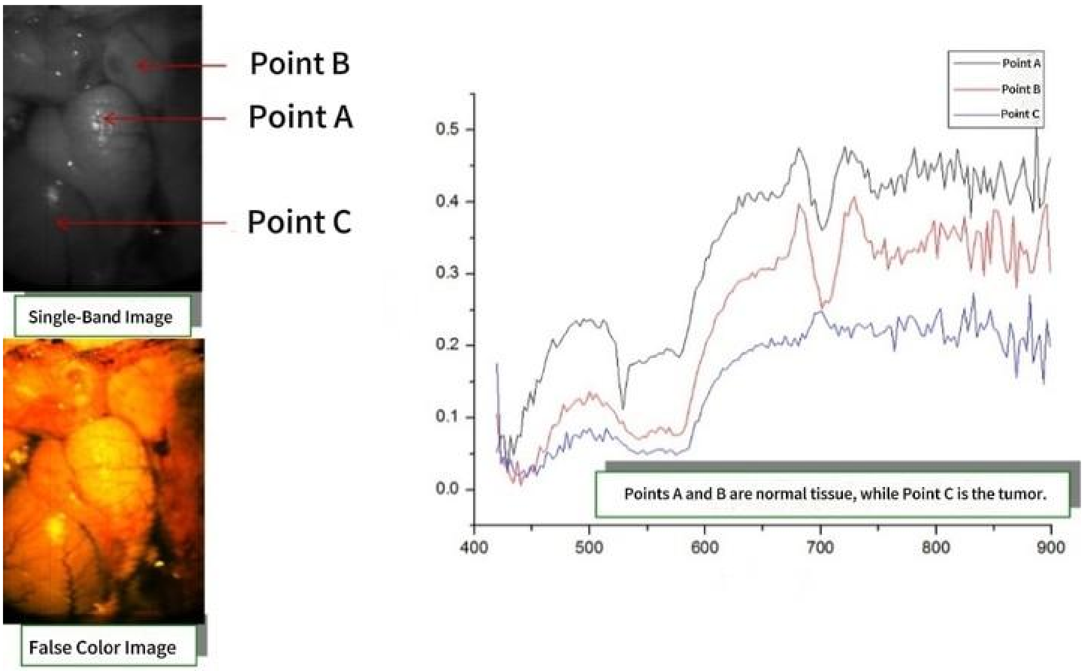

Figure 27 Data from Medical Microscopic Spectral Imager

1503 Bld. A04, 3rd Software Park, Jimei, Xiamen, 361005, China
Tel: +86-592-6102588

5.6. Application in Airborne Imaging Spectroscopy

Application Goal: Airborne Remote Sensing

Application Overview: The figure shows an airborne imaging spectrometer based on SpecVIEW-VIS. The instru ment consists of SpecVIEW-VIS, a stabilization platform, and a POS module. Figures 20 and 21 depict data ac quired during a flight in Jingmen, Hubei, in December 2014. Figure 20 shows a pseudo-color image after geom etric correction, strip stitching, and radiometric calibration. Figure 21 displays the spectral curve of typical groun d objects.

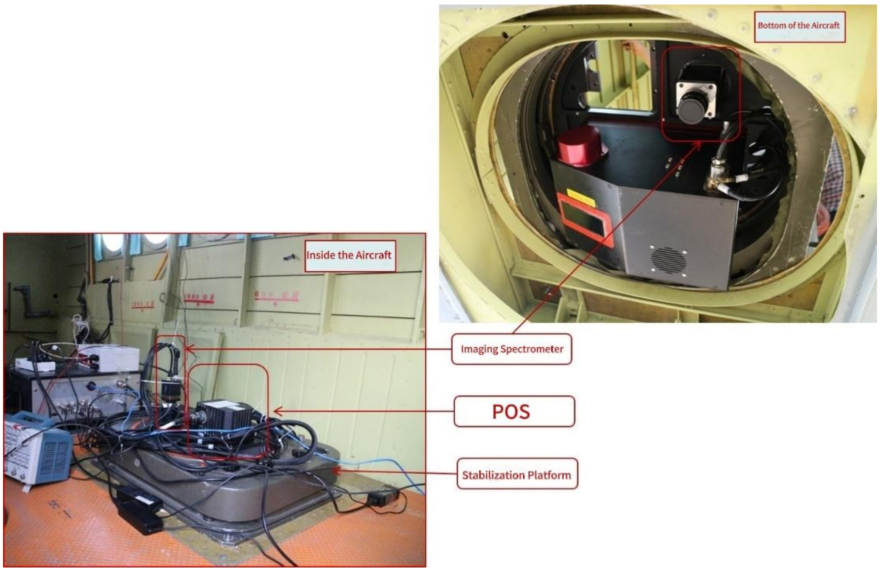

Figure 28 Application of Airborne Remote Sensing

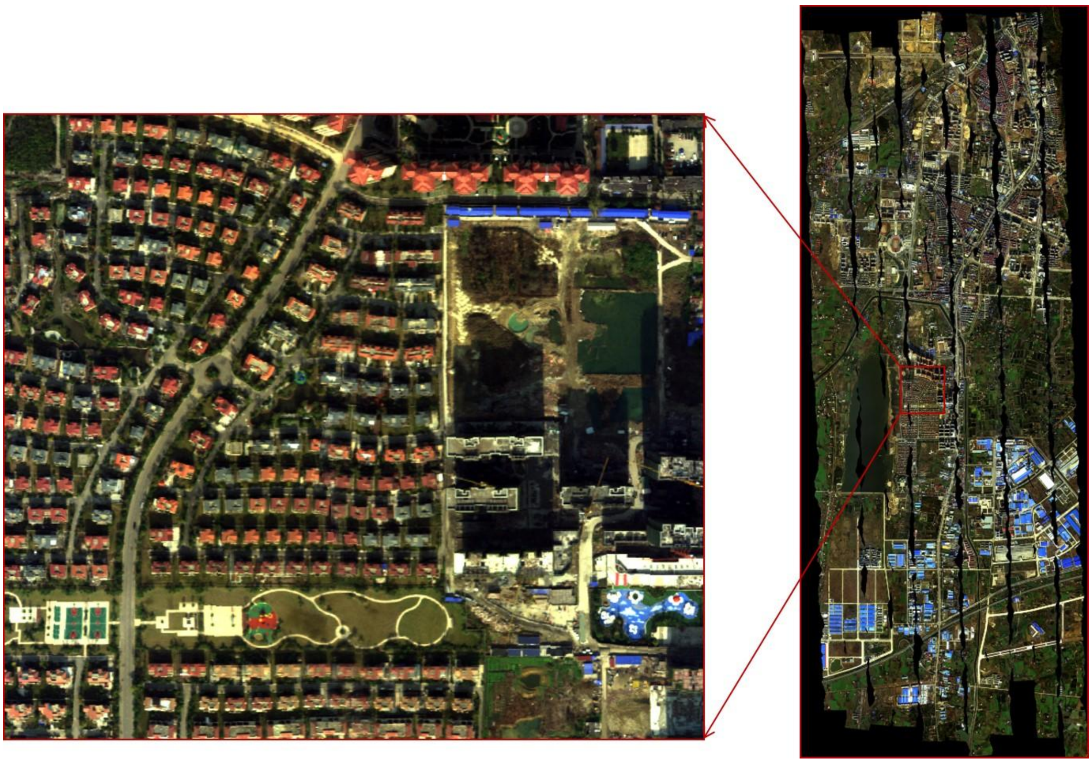

Figure 29 Airborne Application Data — Pseudo-Color Image

1503 Bld. A04, 3rd Software Park, Jimei, Xiamen, 361005, China
Tel: +86-592-6102588

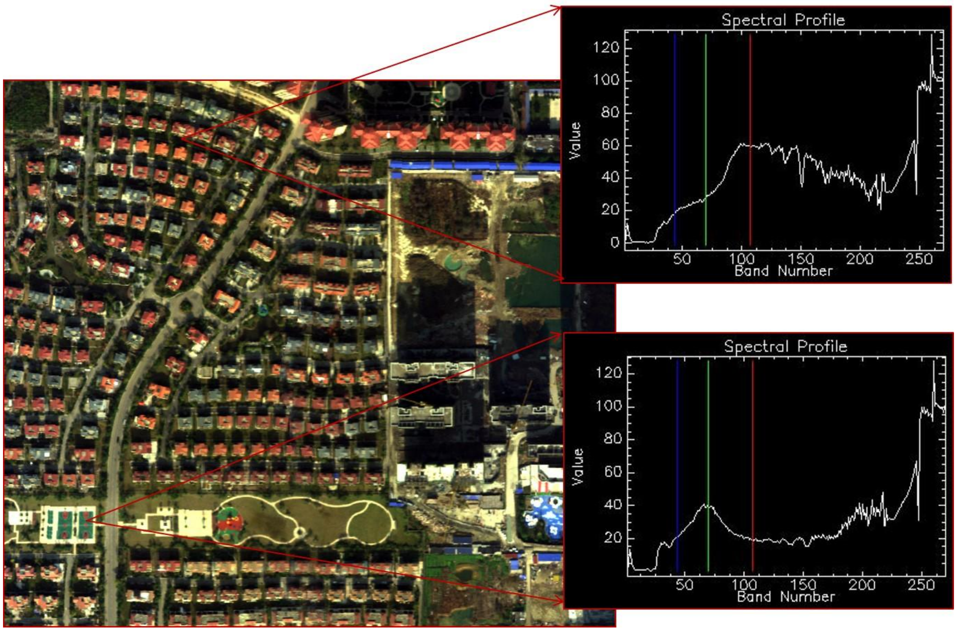

Figure 30 Airborne Application Data — Spectral Curve

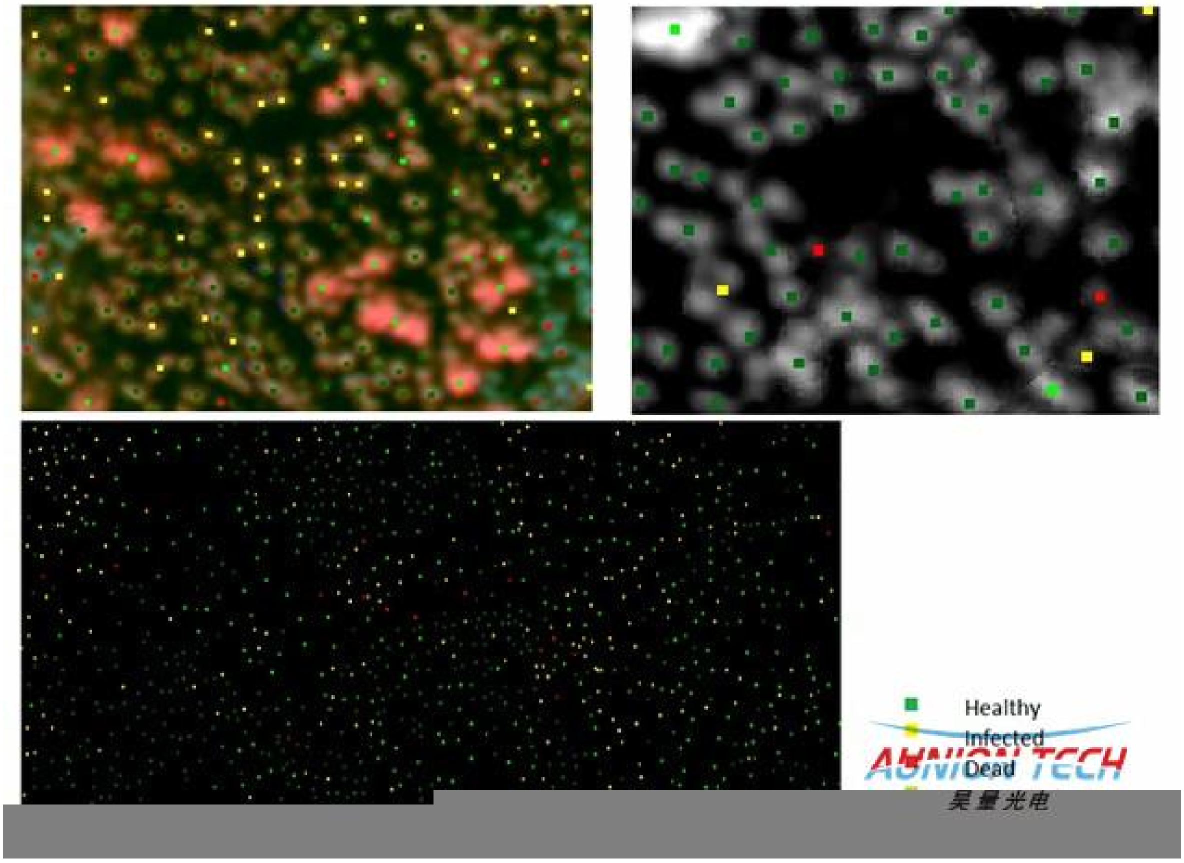

Figure 31 Forest Remote Sensing: Airborne Hyperspectral Observation of Forest Pests and Diseases

1503 Bld. A04, 3rd Software Park, Jimei, Xiamen, 361005, China
Tel: +86-592-6102588

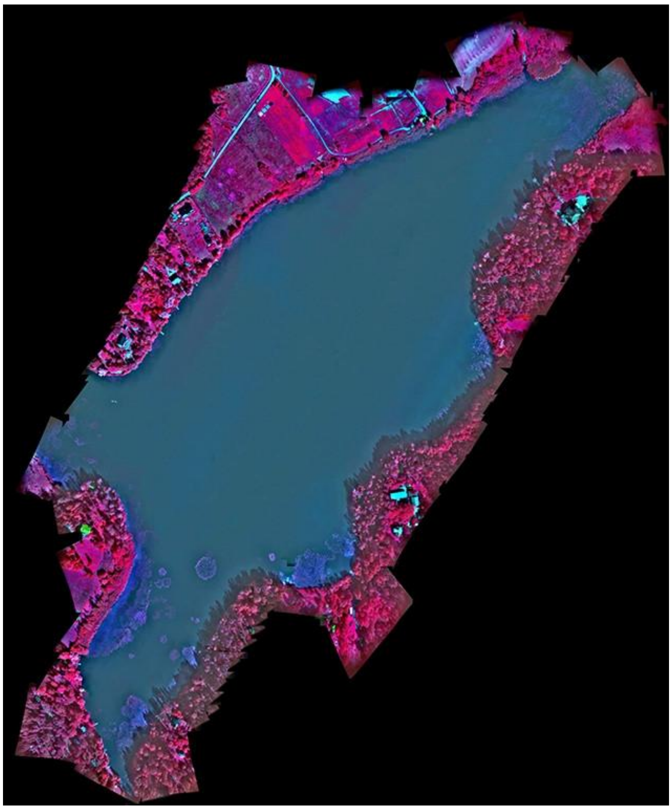

Figure 32 Water Body Detection (Lake Plankton, Algae, Vegetation Research)

1503 Bld. A04, 3rd Software Park, Jimei, Xiamen, 361005, China
Tel: +86-592-6102588